

# Synthesis, In Vitro, and In Silico Studies of *N*-(Substituted-Phenyl)-3-(4-Phenyl-1-Piperazinyl)propanamides as Potent Alkaline Phosphatase Inhibitors

M. A. Abbasi<sup>a, 1</sup>, M. Nazir<sup>a</sup>, Aziz-ur-Rehman<sup>a</sup>, S. Z. Siddiqui<sup>a</sup>, Hussain Raza<sup>b</sup>, Ayesha Zafar<sup>c</sup>, S. A. A. Shah<sup>d</sup>, and M. Shahid<sup>e</sup>

<sup>a</sup> Department of Chemistry, Government College University, Lahore, 54000 Pakistan

<sup>b</sup> College of Natural Sciences, Department of Biological Science, Kongju National University, Gongju, 32588 South Korea

<sup>c</sup> School of Chemical Sciences, University of Auckland, Auckland, 1142 New Zealand

<sup>d</sup> Faculty of Pharmacy and Atta-ur-Rahman Institute for Natural Products Discovery (AuRIns), Level 9, FF3, Universiti Teknologi MARA, Puncak Alam Campus, 42300 Bandar Puncak Alam, Selangor Darul Ehsan, Malaysia

<sup>e</sup> Department of Biochemistry, University of Agriculture, Faisalabad, 38040 Pakistan

Received October 27, 2020; revised November 14, 2020; accepted November 16, 2020

**Abstract**—In the present research work, a new series of *N*-(substituted-phenyl)-3-(4-phenyl-1-piperazinyl)propanamides were synthesized. The synthesis was initiated by the coupling of different aromatic amines with 3-bromopropanoyl chloride in aqueous basic medium, to synthesize different electrophiles with good yields. These electrophiles were further reacted with 1-phenylpiperazine to yield the desired compounds, *N*-(substituted-phenyl)-3-(4-phenyl-1-piperazinyl)propanamides as depicted in scheme 1. The structural confirmation of all the synthesized compounds was corroborated by IR, <sup>1</sup>H NMR, <sup>13</sup>C NMR, HMBC and CHN analysis data. The in vitro inhibitory potential of these propanamides was evaluated against alkaline phosphatase enzyme and it was explored that all these molecules exhibit potent inhibition relative to the standard used. The Kinetics mechanism analyzed by Lineweaver-Burk plots which exposed that *N*-(4-ethylphenyl)-3-(4-phenyl-1-piperazinyl)propanamide inhibited this enzyme competitively by forming an enzyme-inhibitor complex. Moreover, these compounds were studied for cytotoxic behaviour by hemolytic activity, whereby it was avowed that nearly all these propanamides disclosed low cytotoxicity. In addition, kinetic analysis were also carried out to understand the mode of inhibition for these compounds. The in silico investigation of these compounds was also in agreement with the in vitro results. So, it was envisaged that these derivatives might lead to further research gateways for obtaining better and safe as nontoxic medicinal scaffolds for dealing with the alkaline phosphatase related ailments such as bone diseases, diabetes, prostatic cancer and liver dysfunction.

**Keywords:** 1-phenylpiperazine, propanamides, kinetic analysis, alkaline phosphate, molecular docking, cytotoxicity

**DOI:** 10.1134/S1068162021050186

## INTRODUCTION

It is well known that many heterocyclic compounds containing nitrogen and sulfur exhibit different types of bioactivities in a vast variety of medicines including anti-tumor, antibiotic, anti-inflammatory, anti-depressant, anti-malarial, anti-HIV, antiviral, anti-diabetic, herbicidal, anti-fungal, and insecticidal agents. Nitrogen-containing heterocyclic compounds are also known as important class of compounds in medicinal chemistry [1]. Among the nitrogen-containing heterocyclic compounds, piperazine derivatives have shown a wide range of pharmacological properties such as antibacterial activity against resis-

tant pathogens [2], antimalarial activity, dual calcium channel blocking [3], antipsychotic activity, antifungal activity, and antitubercular, anticancer, antiviral, and antioxidant properties [4, 5]. Many commercial drugs, such as the viral protease inhibitor crixivan [6], also contain piperazine derivatives. Among the five- and six-nitrogen heterocyclic compounds, therapeutic agents with high enzyme-inducing activity have been reported [7].

At the present stage of development of organic chemistry, there are lots of basic synthetic approaches to synthesis of propanamides derivatives with a wide spectrum of biological activity. Several propanamides derivatives are reported in literature which show significant anthelmintic, antibacterial, antifungal, anti-

<sup>1</sup> Corresponding author: e-mail: atrabbasi@yahoo.com; abbasi@gcu.edu.pk.

cancer, anticonvulsant, analgesic, anti-allodynic and anti-microbial activity [8–12].

Alkaline phosphatase (AP, EC. 3.1.3.1) belongs to a large family of metal containing phosphatases found in many species from bacteria to man [13]. The 3-D structure of the core of the alkaline phosphatase is strongly conserved among various species (*Escherichia coli* [14, 15]; shrimp [16]; human placenta [17, 18]) as is its catalytic site, with two zinc ions and one magnesium ion. Alkaline phosphatase (ALP) is a critical enzyme in phosphate metabolism due to its ability to catalyze the hydrolysis of phosphoryl esters [19–21]. Moreover, ALP is commonly used as an important biomarker for clinical diagnosis since its abnormal levels is closely associated with many diseases such as bone diseases, diabetes, prostatic cancer and liver dysfunction [22]. Therefore, it is of great importance to develop a sensitive and selective method for ALP detection and its inhibition.

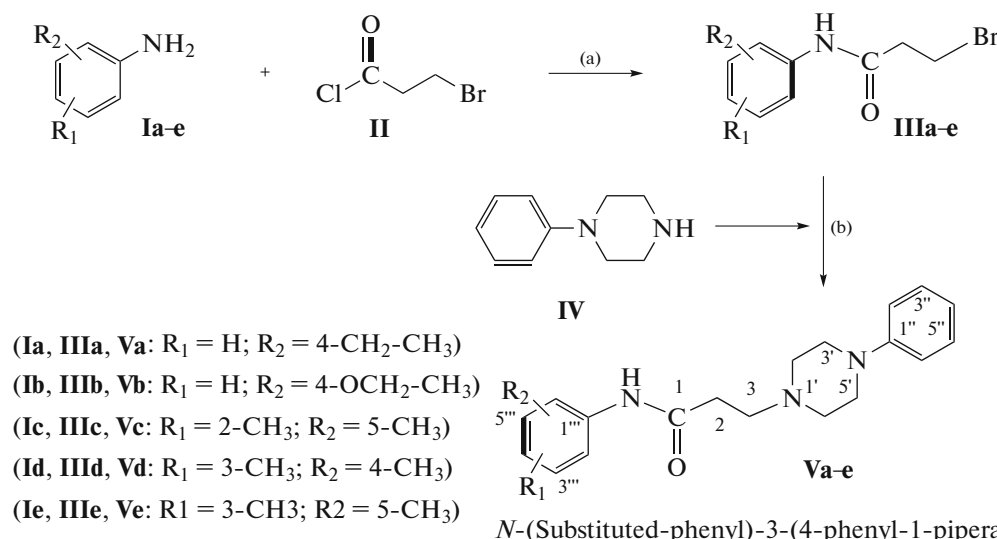
The purpose of our research was to prepare hybrid compounds bearing both propanamide and piperazine moieties to explore their therapeutic potentials as alkaline phosphatase inhibitors. In silico study were also

furnished to ascertain different types of interactions with active pocket of enzyme.

## RESULTS AND DISCUSSION

### Chemistry

The designed *N*-(substituted-phenyl)-3-(4-phenyl-1-piperazinyl)propanamides (**Va-e**), were synthesized through a facile strategy (Scheme 1). The procedures and conditions of the reactions are discussed in the experimental section. The structural confirmation of the synthesized compounds was accomplished using IR, <sup>1</sup>H-NMR, <sup>13</sup>C NMR and CHN analysis techniques. Initially, 3-bromo-*N*-(substituted-phenyl)propanamides (**IIIa-e**) were prepared by the reaction of 3-bromopropanoyl chloride (**II**) with various substituted anilines (**Ia-e**) in 10% aqueous Na<sub>2</sub>CO<sub>3</sub> solution at room temperature. The reaction was consummated by vigorous shaking which gave the desired electrophiles in excellent yield. Then, 1-phenylpiperazine (**IV**) was coupled with the newly synthesized electrophiles (**IIIa-e**) to achieve a series of new *N*-(substituted-phenyl)-3-(4-phenyl-1-piperazinyl)propanamides (**Va-e**).



**Scheme 1.** Protocol for the synthesis of *N*-(substituted-phenyl)-3-(4-phenyl-1-piperazinyl)propanamides (**Va-e**). Reagents & Conditions: (a) Aq. Na<sub>2</sub>CO<sub>3</sub> soln./pH 9–10/vigorous shaking at RT for 20–30 minutes. (b) (**IV**)/DMF/LiH/stirring at RT for 0.5 hrs for activation of (**IV**) and then addition of electrophiles (**IIIa-e**) (one in each reaction), followed by stirring for 15–16 hrs.

One of the compounds (**Vb**) is discussed hereby in detail for the pragmatism of the readers. It was obtained as violet solid with yield 89% and melting point 158–159°C. Its molecular formula, C<sub>21</sub>H<sub>27</sub>N<sub>3</sub>O<sub>2</sub> was ascribed by counting the number of proton in its <sup>1</sup>H NMR spectrum. The CHN analysis data was also in agreement with its molecular formula, C<sub>21</sub>H<sub>27</sub>N<sub>3</sub>O<sub>2</sub>. Presence of different functional group was ascertained by

the IR spectral data. The absorption band at 3339 cm<sup>-1</sup> was characteristic of N–H stretching. The other bands were observed at 3086 (C–H, str. of aromatic ring), 2905 (C–H, aliphatic str.), 1680 (aromatic C=C stretching), 1654 (C=O str.) cm<sup>-1</sup>. With the help of <sup>1</sup>H NMR spectrum of this molecule, the 4-ethoxyphenyl ring attached at the nitrogen atom of propanamide moiety was identified clearly by the characteris-

tic signals at 7.46 (br.d,  $J = 8.8$ , 2H, H-2'' & H-6'''), 6.85 (br.d,  $J = 8.7$ , 2H, H-3'' & H-5'''), 3.96 (q,  $J = 6.8$  Hz, 2H, CH<sub>3</sub>-CH<sub>2</sub>-O-4''') and 1.29 (t,  $J = 6.9$ , 3H, CH<sub>3</sub>-CH<sub>2</sub>-O-4''') ppm. A highly deshielded singlet appearing at  $\delta$  9.92 ppm was assigned to -NH proton of propanamide group (-NHCO). The two triplets for adjacent methylenes resonating at  $\delta$  2.67 (t,  $J = 7.0$ , 2H, CH<sub>2</sub>-2) and 2.47 (t,  $J = 6.9$ , 2H, CH<sub>2</sub>-3) ppm were peculiar for the propanamidic entity. Similarly, the signals of a phenyl ring attached with piperazine were rational in the aromatic region at  $\delta$  7.20 (br.t,  $J = 7.6$  Hz, 2H, H-3'' and H-5''), 6.92 (br.d,  $J = 8.1$  Hz, 2H, H-2'' and H-6''), and 6.77 (br.t,  $J = 7.2$ , 1H, H-4''), while the signals of pseudo-symmetrical 1,4-piperazine unit were observed in aliphatic region at  $\delta$  3.12 (br.s, 4H, CH<sub>2</sub>-3' and CH<sub>2</sub>-5') and 2.57-2.56 (m, 4H, CH<sub>2</sub>-2' and CH<sub>2</sub>-6'). The <sup>1</sup>H-NMR spectrum of this compound is shown in Fig. S1(a-c).

In the <sup>13</sup>C NMR spectrum (Fig. S2), the 4-ethoxyphenyl moiety of ring attached to propanamido group was verified by four discrete resonances in aromatic region at  $\delta$  154.27 (C-4'''), 132.28 (C-1'''), 120.52 (C-2'' and C-6''') and 114.33 (C-3'' and C-5'''), and two signals in aliphatic region appeared at  $\delta$  63.03 (CH<sub>3</sub>-CH<sub>2</sub>-O-4''') and 14.65 (CH<sub>3</sub>-CH<sub>2</sub>-O-4'''). The propanamide group showed peaks at  $\delta$  169.56 (C-1), 53.79 (C-3) and 33.95 (C-2). The phenyl ring attached to the nitrogen atom of piperazine was obvious by four signals  $\delta$  150.95 (C-1''), 128.85 (C-3'' and C-5''), 118.75 (C-4'') and 115.31 (C-2'' and C-6''). The pseudo-symmetrical piperazine heterocycle was corroborated by two signals at  $\delta$  52.40 (C-2' and C-6') and 48.18 (C-3' and C-5'). The salient connectivity's in the carbon skeleton of this molecule were thoroughly verified by its HMBC spectrum. This spectrum, along with significant correlations, is shown in Fig. S3. So, on account of aforementioned evidences, the structure of molecule (Vb) was confirmed as *N*-(4-ethoxyphenyl)-3-(4-phenyl-1-piperazinyl)propanamide. A similar design was implemented for the structural characterization of other derivatives (Fig. S4-S11) in the synthesized series.

### Pharmacology

**Alkaline phosphatase inhibition and structure-activity relationship.** The synthesized *N*-phenylpiperazine bearing propanamides, (Va-e) were investigated against alkaline phosphate and their inhibitory potentials are tabulated in Table 1. These molecules exhibited very excellent activities, as evident from their lower IC<sub>50</sub> ( $\mu$ M) values, relative to standard, KH<sub>2</sub>PO<sub>4</sub>, having IC<sub>50</sub> value of  $5.242 \pm 0.473 \mu$ M. The general

structural units of the examined compounds are labeled in Fig. 1.

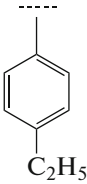
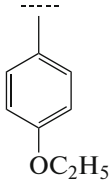
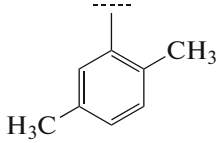
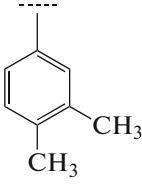
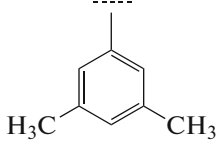
When the inhibitory potential of *para*-substituted (aryl part) molecules was compared, it was observed that (Va) with *para*-ethyl group had a better activity (IC<sub>50</sub> =  $0.531 \pm 0.003 \mu$ M), relative to (Vb) (IC<sub>50</sub> =  $2.571 \pm 0.075 \mu$ M) bearing a *para*-ethoxy group, probably due to the reason that in former molecule the non-polar and comparatively smaller ethyl group penetrated well in the active site and interacted in a better way with the enzyme (Fig. 2). Anyhow, both these molecules were much better inhibitors than the standard, KH<sub>2</sub>PO<sub>4</sub> (IC<sub>50</sub> =  $5.242 \pm 0.473 \mu$ M).

When the inhibitory potential of three di-methylated regio-isomers was compared, it was observed that the compound (Vc) having methyl groups at *ortho* and *meta* positions possessed superior inhibitory activity (IC<sub>50</sub> =  $2.361 \pm 0.044 \mu$ M) as compared to (Ve) (IC<sub>50</sub> =  $2.361 \pm 0.044 \mu$ M) and (Vd) (IC<sub>50</sub> =  $7.118 \pm 0.817 \mu$ M). It indicated that the molecule bearing the methyl groups sterically away from each other in the aryl part was more prone to have better interactions with the enzyme relative to other analogues (Fig. 3).

**Hemolytic activity.** To determine the cytotoxicity of the synthesized propanamides, (Va-e), these were subjected to hemolytic assay. Percentage hemolysis (%) results are given in Table 1. According to the results, almost all these derivatives showed mild cytotoxicity towards RBC plasma membrane. Compound (Ve) (7.38%) showed maximum membrane cytotoxicity while (Vd) (0.86%) rendered minimum membrane toxicity amongst the series. In principle, the other molecules (Va) (1.75%) (Vb) (4.72%), and (Vc) (3.27%) also exhibited much lower cytotoxicity as compared to the standard Triton-X (89.39%).

**Kinetic mechanism.** Presently, the most potent compound (Va) was studied for their mode of inhibition against alkaline phosphatase. The potential of this compound to inhibit the free enzyme and enzyme-substrate complex was determined in terms of EI and ESI constants respectively. The kinetic studies of the enzyme by the Lineweaver-Burk plot of 1/V versus substrate *para*-nitrophenyl phosphate disodium salt 1/[S] in the presence of different inhibitor concentrations gave a series of straight lines as shown in Fig. 7a. The results of compound (Va) showed that it intersected within the second quadrant. The analysis showed that  $V_{max}$  decreased to new increasing doses of inhibitors on the other hand  $K_m$  remained the same. This behavior indicated that (Va) inhibited the alkaline phosphatase non-competitively to form enzyme-inhibitor complex. Secondary plot of slope against the concentration of inhibitors showed enzyme-inhibitor

**Table 1.** Alkaline phosphatase inhibitory activity of (Va–e) series

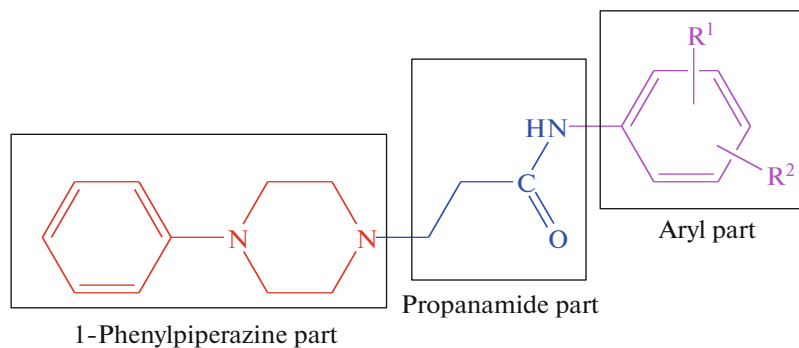
Compound	Aryl Part	Alkaline phosphatase IC <sub>50</sub> , μM	Hemolysis, %
(Va)		0.531 ± 0.003	1.75 ± 0.035
(Vb)		2.571 ± 0.075	4.72 ± 0.08
(Vc)		2.162 ± 0.017	3.27 ± 0.02
(Vd)		7.118 ± 0.817	0.86 ± 0.023
(Ve)		2.361 ± 0.044	7.38 ± 0.04
Standards		<b>KH<sub>2</sub>PO<sub>4</sub></b> 5.242 ± 0.473	<b>Triton X</b> 89.39 ± 0.67 <b>PBS</b> 0.47 ± 0.018

Values are presented as mean ± SEM (standard error of mean).

dissociation constant ( $K_i$ ) Fig. 4b. The kinetic results are presented in Table 2.

**Molecular modelling.** Molecular modeling studies were carried out to determine the plausible binding modes of potent inhibitors in crystal structures of

alkaline phosphatase (AP) [18], using GOLD software [23], and all the ligands fitted into the pocket in a similar way with reasonable predicted affinity for the scoring functions used as can be seen in Table 3. As can be seen in Table 4, that high GoldScore and ChemPLP

**Fig. 1.** General structural features of compounds (Va–e).

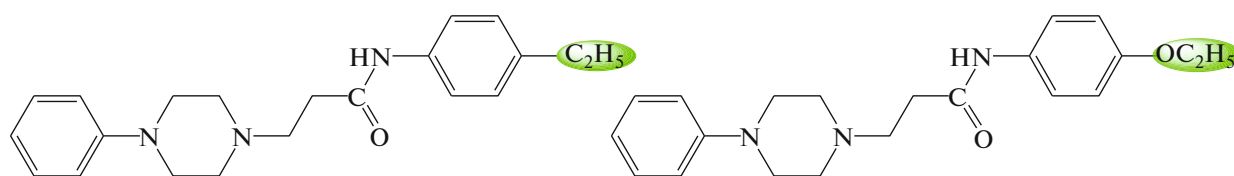


Fig. 2. Structure-activity relationships of compounds, (Va) and (Vb).

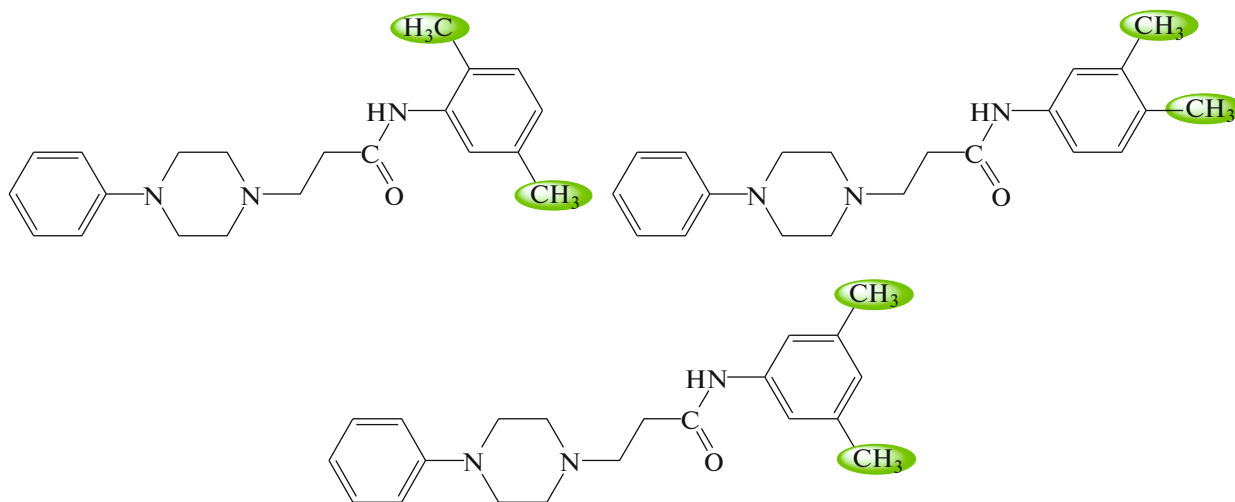


Fig. 3. Structure-activity relationships of compounds, (Vc), (Vd) and (Ve).

were observed for (Va) ligand as compared to most of other molecules in the series, which is consistent with its experimental  $IC_{50}$  value. The ChemScore and ASP values were also considerable for this molecule.

Detailed binding site interactions of the most active inhibitor (Va) ( $IC_{50} = 0.531 \pm 0.003 \mu\text{M}$ ) are indicated

in Figs. 5a, 5b. Rest of docked compounds is mentioned in the supplementary data Figs. S12–S15. The compound (Va) blocked the catalytically active zinc and magnesium ions site and exhibited hydrogen bonding interaction with side chains of Arg166 through nitrogen atom of piperazinyl moiety. The eth-

**Table 2.** Kinetic parameters of the alkaline phosphatase for *para*-nitrophenylphosphate disodium salt activity in the presence of different concentrations of (Va)

Concentration, $\mu\text{M}$	$V_{\text{max}}$ , $\Delta\text{A}/\text{min}$	$K_m$ , mM	Inhibition Type	$K_i$ , $\mu\text{M}$
0.00	0.00163	0.263	Non-competitive	0.5
0.531	0.00119	0.263		
1.062	0.00067	0.263		

$V_{\text{max}}$ , the reaction velocity.  
 $K_m$ , Michaelis-Menten constant;  
 $K_i$ , EI dissociation constant.

**Table 3.** The results of the scoring functions and interactions for the compounds (Va–e)

Compound	GS	CS	Chem PLP	ASP	H-Bonding (HB)	Lipophilic contacts (LC)
(Va)	58.9	25.8	68.0	28.1	Arg166	His153, His317, His320, His432
(Vb)	59.9	24.9	67.9	29.5	–	His317, His320, Glu429, Val89
(Vc)	55.7	24.6	66.9	26.6	–	Lys87, His432, His320, His317, His153, Phe107
(Vd)	56.2	25.1	66.6	28.3	–	His317, His432, Phe107
(Ve)	58.9	24.8	66.3	27.5	His317	His432, His320

Values are presented as Mean  $\pm$  SEM (Standard error of mean).

**Table 4.** Calculated molecular descriptors for the alkaline phosphatase inhibitors (**Va–e**)

Compound	MW, g/mol	HD	HA	Log P	PSA, Å <sup>2</sup>	RB
( <b>Va</b> )	337	1	5.5	4.1	47.521	5
( <b>Vb</b> )	353	1	6.3	4.1	56.322	6
( <b>Vc</b> )	337	1	5.5	4.1	47.521	4
( <b>Vd</b> )	337	1	5.5	3.9	47.521	4
( <b>Ve</b> )	337	1	5.5	4.1	47.521	4

ylphenyl moiety of the ligand is embedded deeply in hydrophobic pocket, interacting with His432 via  $\pi$ – $\pi$  stacking. The phenylpiperazinyl moiety sits aside the pocket, interacting with the His320, His317, and His153. The similarities in the docked configurations to the one described in the literature suggested the reliability and reproducibility of the docking protocol [24–26].

The calculated molecular descriptors (MW, molecular weight; LogP octanol, water partition coefficient; HD, hydrogen bond donors; HA, hydrogen bond acceptors; PSA, polar surface area; given in Table 4. The ligands are relatively average in size with molecular weight between 337 and 353 and lie in the *lead-like space* (for definition of lead-like, drug-like and Known Drug Space regions) [27]. The logP values range from 3.9 to 4.1. They all are within the boundaries of *lead-like space*. Moreover, the PSA values also indicated that they all lie in the *lead-like space*.

## EXPERIMENTAL

### General

Chemicals were purchased from Sigma Aldrich & Alfa Aesar (Germany) and solvents of analytical grades were supplied by local suppliers. By using open capillary tube method, melting points were taken on

Griffin and George apparatus and were uncorrected. By using thin layer chromatography (with ethyl acetate and *n*-hexane (30 : 70) as mobile phase), initial purity of compounds was detected at 254 nm. IR peaks were recorded on a Jasco-320-A spectrometer by using KBr pellet method. <sup>1</sup>H NMR signals were recorded at 600 MHz and <sup>13</sup>C NMR at 150 MHz in DMSO-*d*<sub>6</sub> using Bruker spectrometers.

**Preparation of 3-bromo-*N*-(substituted-phenyl)propanamides (**IIIa–e**).** Preparation of various 3-bromo-*N*-(substituted-phenyl)propanamides was carried out by reaction of various aryl amines (**Ia–e**) with 3-bromopropanoyl chloride (**II**) in equimolar quantities (0.001 moles) and shaking manually but vigorously in 10% aqueous Na<sub>2</sub>CO<sub>3</sub> solution. Solid precipitates were formed after 20–30 minutes, which were filtered and washed with cold distilled water to obtain the desired electrophiles, (**IIIa–e**). The physical data of all these electrophiles was in agreement with reported literature [28].

**General procedure for the synthesis of *N*-(substituted-phenyl)-3-(4-phenyl-1-piperazinyl)propanamides (**Va–e**).** 1-Phenyl piperazine (**IV**), (0.2 g; 1.0 mmol) was dispersed in about 5 mL DMF and one pinch of LiH, contained in a 50 mL round bottomed (RB) flask and the mixture was stirred for about

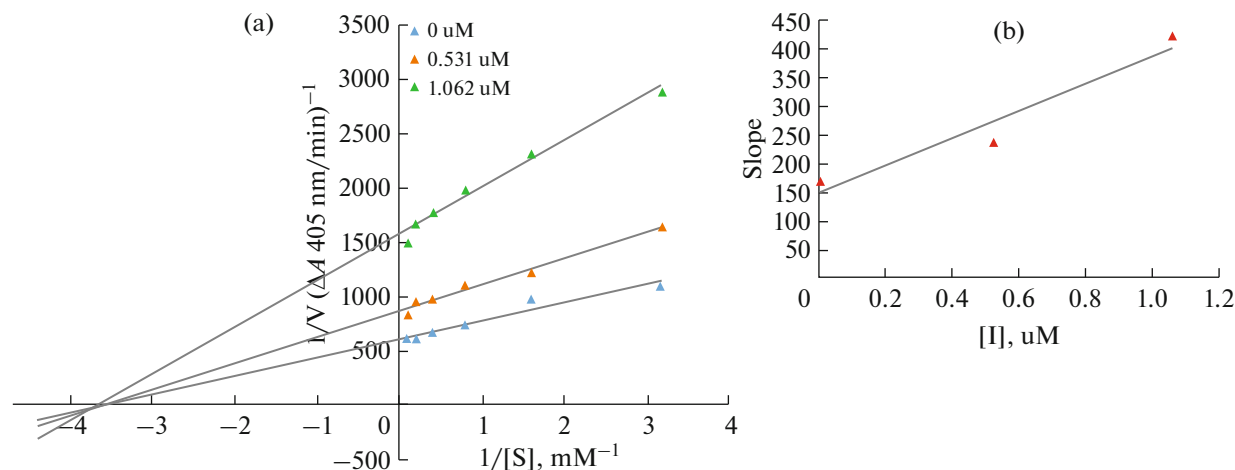


**Fig. 4.** Lineweaver–Burk plots for inhibition of alkaline phosphatase in the presence of compound (**Va**). Concentrations of (**Va**) were 0.00, 0.531 and 1.062  $\mu$ M (A), The insets represent the plot of the slope versus inhibitor (**Va**) concentrations to determine inhibition constant. The lines were drawn using linear least squares fit (B).

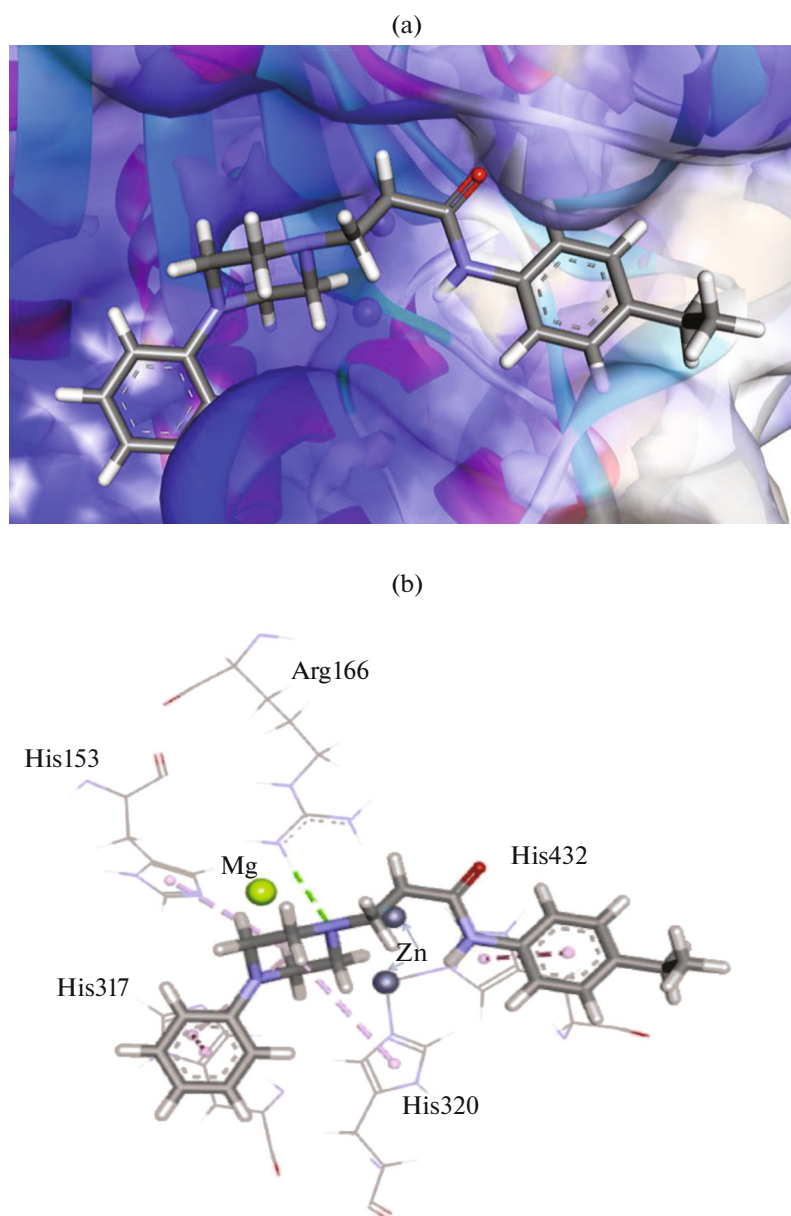


**Fig. 5.** Docked configuration of (**Va**) to alkaline phosphatase (AP) (PDB ID: 1ZED) using GS. The surface is rendered. Blue and white depict hydrophilic and hydrophobic areas respectively (a), predicted hydrogen bonding and lipophilic contacts are indicated by green (HB) and purple (LC) dashed lines (b).

30 minutes. Then, calculated equimolar amounts of 3-bromo-*N*-(substituted-phenyl)propanamides (**IIIa–e**; one in each reaction) were added and the reaction mixture was stirred for 15–16 hours. The completion of the reaction was monitored with TLC, and when single spot obtained, ice chilled distilled water was added drop wise in the reaction solution until the product was precipitated. These precipitates were filtered, washed with distilled water and dried to obtain the desired products. All the compounds were re-crystallized from methanol.

***N*-(4-Ethylphenyl)-3-(4-phenyl-1-piperazinyl)propanamide (Va).** Orange amorphous solid; yield: 91%; mp 136–137°C; molecular formula: C<sub>21</sub>H<sub>27</sub>N<sub>3</sub>O; IR (KBr),  $\nu$  (cm<sup>-1</sup>): 3328 (N–H, stretching), 3081 (C–H, str. of aromatic ring), 2905 (–CH<sub>2</sub> stretching), 1688 (aromatic C=C stretching), 1648 (C=O str.); <sup>1</sup>H NMR (600 MHz, DMSO-*d*<sub>6</sub>):  $\delta$  10.04 (s, 1H, NH), 7.51 (br.d, *J* = 8.1, 2H, H-2''' and H-6'''), 7.20 (br.t, *J* = 7.7 Hz, 2H, H-3'' and H-5'''), 7.13 (br.d, *J* = 8.1, 2H, H-3''' and H-5'''), 6.92 (br.d, *J* = 8.1 Hz, 2H, H-2'' and H-6''), 6.77 (br.t, *J* = 7.1, 1H, H-4''), 3.12 (br.s, 4H, CH<sub>2</sub>-3' and CH<sub>2</sub>-5'), 2.69 (t, *J* = 6.9, 2H, CH<sub>2</sub>-2), 2.57 (br.s,



4H, CH<sub>2</sub>-2' and CH<sub>2</sub>-6'), 2.54–2.50 (m, 4H, CH<sub>2</sub>-3 and CH<sub>3</sub>-CH<sub>2</sub>-4'''), 1.14 (t, *J* = 7.5, 3H, CH<sub>3</sub>-CH<sub>2</sub>-4'''); <sup>13</sup>C NMR (150 MHz, DMSO-*d*<sub>6</sub>): δ 169.87 (C-1), 150.94 (C-1''), 138.38 (C-1'''), 136.91 (C-4'''), 128.84 (C-3'' and C-5'''), 127.81 (C-2'' and C-6'''), 119.11 (C-3''' and C-5'''), 118.74 (C-4''), 115.30 (C-2'' and C-6''), 53.77 (C-3), 52.41 (C-2' and C-6'), 48.20 (C-3' and C-5'), 34.06 (C-2), 27.57 (CH<sub>3</sub>-CH<sub>2</sub>-4'''), 15.68 (CH<sub>3</sub>-CH<sub>2</sub>-4''); Anal. Calc. for C<sub>21</sub>H<sub>27</sub>N<sub>3</sub>O (337.22): C, 74.74; H, 8.06; N, 12.45. Found: C, 74.70; H, 8.01; N, 12.41.

***N*-(4-Ethoxyphenyl)-3-(4-phenyl-1-piperazinyl)propanamide (Vb).** Violet amorphous solid; yield: 89%; mp 158–159°C; molecular formula: C<sub>21</sub>H<sub>27</sub>N<sub>3</sub>O<sub>2</sub>; IR (KBr), ν (cm<sup>-1</sup>): 3339 (N–H, stretching), 3086 (C–H, str. of aromatic ring), 2905 (–CH<sub>2</sub> stretching), 1680 (aromatic C=C stretching), 1654 (C=O str.); <sup>1</sup>H NMR (600 MHz, DMSO-*d*<sub>6</sub>): δ 9.92 (s, 1H, NH), 7.46 (br.d, *J* = 8.8, 2H, H-2'' and H-6'''), 7.20 (br.t, *J* = 7.6 Hz, 2H, H-3'' and H-5'''), 6.92 (br.d, *J* = 8.1 Hz, 2H, H-2'' and H-6''), 6.85 (br.d, *J* = 8.7, 2H, H-3''' and H-5'''), 6.77 (br.t, *J* = 7.2, 1H, H-4''), 3.96 (q, *J* = 6.8 Hz, 2H, CH<sub>3</sub>-CH<sub>2</sub>O-4'''), 3.12 (br.s, 4H, CH<sub>2</sub>-3' and CH<sub>2</sub>-5'), 2.67 (t, *J* = 7.0, 2H, CH<sub>2</sub>-2), 2.57–2.56 (m, 4H, CH<sub>2</sub>-2' and CH<sub>2</sub>-6'), 2.47 (t, *J* = 6.9, 2H, CH<sub>2</sub>-3), 1.29 (t, *J* = 6.9, 3H, CH<sub>3</sub>-CH<sub>2</sub>O-4''); <sup>13</sup>C NMR (150 MHz, DMSO-*d*<sub>6</sub>): δ 169.56 (C-1), 154.27 (C-4'''), 150.95 (C-1''), 132.28 (C-1'''), 128.85 (C-3'' and C-5'''), 120.52 (C-2'' and C-6'''), 118.75 (C-4''), 115.31 (C-2'' and C-6''), 114.33 (C-3''' and C-5'''), 63.03 (CH<sub>3</sub>-CH<sub>2</sub>O-4'''), 53.79 (C-3), 52.40 (C-2' and C-6'), 48.18 (C-3' and C-5'), 33.95 (C-2), 14.65 (CH<sub>3</sub>-CH<sub>2</sub>O-4''); Anal. Calc. for C<sub>21</sub>H<sub>27</sub>N<sub>3</sub>O<sub>2</sub> (353.21): C, 71.36; H, 7.70; N, 11.89. Found: C, 71.30; H, 7.65; N, 12.85.

***N*-(2,5-Dimethylphenyl)-3-(4-phenyl-1-piperazinyl)propanamide (Vc).** Purple amorphous solid; yield: 91%; mp 140–141°C; Molecular formula: C<sub>21</sub>H<sub>27</sub>N<sub>3</sub>O; IR (KBr), ν (cm<sup>-1</sup>): 3342 (N–H, stretching), 3081 (C–H, str. of aromatic ring), 2905 (–CH<sub>2</sub> stretching), 1677 (aromatic C=C stretching), 1652 (C=O str.); <sup>1</sup>H-NMR (600 MHz, DMSO-*d*<sub>6</sub>): δ 9.49 (s, 1H, NH), 7.37 (br.s, 1H, H-6'''), 7.20 (br.t, *J* = 8.1 Hz, 2H, H-3'' and H-5'''), 7.05 (br.d, *J* = 7.6 Hz, 1H, H-3'''), 6.94 (br.d, *J* = 8.2 Hz, 2H, H-2'' and H-6''), 6.86 (br.d, *J* = 7.4 Hz, 1H, H-4'''), 6.77 (br.t, *J* = 7.2, 1H, H-4''), 3.14–3.13 (m, 4H, CH<sub>2</sub>-3' and CH<sub>2</sub>-5'), 2.68 (t, *J* = 6.6, 2H, CH<sub>2</sub>-2), 2.61–2.59 (m, 4H, CH<sub>2</sub>-2' and CH<sub>2</sub>-6'), 2.53 (t, *J* = 6.6, 2H, CH<sub>2</sub>-3), 2.23 (s, 3H, CH<sub>3</sub>-5'''), 2.16 (s, 3H, CH<sub>3</sub>-2'''); <sup>13</sup>C-NMR (150 MHz, DMSO-*d*<sub>6</sub>): δ 170.02 (C-1), 150.92 (C-1''), 136.30 (C-1'''), 134.85 (C-2'''), 129.94 (C-3'''), 128.87 (C-3'' and C-5'''), 127.40 (C-5'''), 125.28 (C-4'''), 124.66 (C-6'''), 118.80 (C-4''), 115.31 (C-2'' and C-6''), 53.96 (C-3), 52.42 (C-2' and C-6'), 48.11 (C-3' and C-5'), 33.41 (C-2), 20.63 (CH<sub>3</sub>-5'''), 17.67 (CH<sub>3</sub>-2''); Anal. Calc. for C<sub>21</sub>H<sub>27</sub>N<sub>3</sub>O (337.22): C, 74.74; H, 8.06; N, 12.45. Found: C, 74.69; H, 8.00; N, 12.39.

***N*-(3,4-Dimethylphenyl)-3-(4-phenyl-1-piperazinyl)propanamide (Vd).** White amorphous solid; yield: 73%; mp 96–97°C; molecular formula: C<sub>21</sub>H<sub>27</sub>N<sub>3</sub>O; molecular weight: 337 g/mol; IR (KBr), ν (cm<sup>-1</sup>): 3340 (N–H, stretching), 3080 (C–H, str. of aromatic ring), 2900 (–CH<sub>2</sub> stretching), 1670 (aromatic C=C stretching), 1647 (C=O str.); <sup>1</sup>H NMR (600 MHz, DMSO-*d*<sub>6</sub>): δ 9.95 (s, 1H, NH), 7.40 (br.s, 1H, H-2'''), 7.34 (br.d, *J* = 7.6 Hz, 1H, H-6'''), 7.20 (br.t, *J* = 7.5 Hz, 2H, H-3'' and H-5'''), 7.04 (br.d, *J* = 7.4 Hz, 1H, H-5'''), 6.91 (br.d, *J* = 7.9 Hz, 2H, H-2'' and H-6''), 6.77 (br.t, *J* = 7.0, 1H, H-4''), 3.11 (br.s, 4H, CH<sub>2</sub>-3' and CH<sub>2</sub>-5'), 2.69 (dist.t, *J* = 6.7, 2H, CH<sub>2</sub>-2), 2.56 (br.s, 4H, CH<sub>2</sub>-2' and CH<sub>2</sub>-6'), 2.51 (dist.t, *J* = 6.6, 2H, CH<sub>2</sub>-3), 2.18 (s, 3H, CH<sub>3</sub>-4'''), 2.15 (s, 3H, CH<sub>3</sub>-3'''); <sup>13</sup>C NMR (150 MHz, DMSO-*d*<sub>6</sub>): δ 169.81 (C-1), 150.94 (C-1''), 136.98 (C-3'''), 136.16 (C-1'''), 130.66 (C-4'''), 129.48 (C-5'''), 128.84 (C-3'' and C-5'''), 120.28 (C-2'''), 118.74 (C-4''), 116.59 (C-6'''), 115.29 (C-2'' and C-6''), 53.81 (C-3), 52.42 (C-2' and C-6'), 48.19 (C-3' and C-5'), 34.09 (C-2), 19.57 (CH<sub>3</sub>-4'''), 18.71 (CH<sub>3</sub>-3'''); Anal. Calc. for C<sub>21</sub>H<sub>27</sub>N<sub>3</sub>O (337.22): C, 74.74; H, 8.06; N, 12.45. Found: C, 74.70; H, 8.02; N, 12.40.

***N*-(3,5-Dimethylphenyl)-3-(4-phenyl-1-piperazinyl)propanamide (Ve).** Yellow amorphous solid; yield: 93%; mp 98–93°C; molecular formula: C<sub>21</sub>H<sub>27</sub>N<sub>3</sub>O; molecular weight: 337 g/mol; IR (KBr), ν (cm<sup>-1</sup>): 3336 (N–H, stretching), 3074 (C–H, str. of aromatic ring), 2895 (–CH<sub>2</sub> stretching), 1683 (aromatic C=C stretching), 1656 (C=O str.); <sup>1</sup>H NMR (600 MHz, DMSO-*d*<sub>6</sub>): δ 9.95 (s, 1H, NH), 7.27 (br.s, 2H, H-2'' and H-6'''), 7.21 (br.t, *J* = 7.2 Hz, 2H, H-3'' and H-5'''), 6.92 (br.d, *J* = 9.3 Hz, 2H, H-2'' and H-6''), 6.78 (br.t, *J* = 6.7, 1H, H-4''), 6.67 (br.s, 1H, H-4'''), 3.11 (br.s, 4H, CH<sub>2</sub>-3' and CH<sub>2</sub>-5'), 2.69–2.68 (m, 2H, CH<sub>2</sub>-2), 2.56 (br.s, 4H, CH<sub>2</sub>-2' and CH<sub>2</sub>-6'), 2.52 (dist.t, *J* = 6.4, 2H, CH<sub>2</sub>-3), 2.23 (s, 6H, CH<sub>3</sub>-3'' and CH<sub>3</sub>-5''); <sup>13</sup>C NMR (150 MHz, DMSO-*d*<sub>6</sub>): δ 169.96 (C-1), 150.94 (C-1''), 139.11 (C-1'''), 137.56 (C-3'' and C-5'''), 128.83 (C-3'' and C-5'''), 124.53 (C-4'''), 118.73 (C-4''), 116.81 (C-2'' and C-6'''), 115.29 (C-2'' and C-6''), 53.81 (C-3), 52.44 (C-2' and C-6'), 48.20 (C-3' and C-5'), 34.19 (C-2), 21.08 (CH<sub>3</sub>-3'' and CH<sub>3</sub>-5''); Anal. Calc. for C<sub>21</sub>H<sub>27</sub>N<sub>3</sub>O (337.22): C, 74.74; H, 8.06; N, 12.45. Found: C, 74.72; H, 8.02; N, 12.40.

### Pharmacology

**Alkaline phosphatase inhibition assay.** Activity of calf intestinal alkaline phosphatase (CIALP) was measured by spectrophotometric assay as previously described by [29, 30]. The reaction mixture comprised of 50 mM Tris-HCl buffer (5 mM MgCl<sub>2</sub>, 0.1 mM ZnCl<sub>2</sub> pH 9.5), the compound (0.1 mM with final DMSO 1% (v/v) and mixture was pre-incubated for 10 min by adding 5 μL of CIALP (0.025 U/mL). Then, 10 μL of substrate (0.5 mM *p*-NPP (para nitro-



phenylphosphate disodium salt) was added to initiate the reaction and the assay mixture was incubated again for 30 min at 37°C. The change in absorbance of released *p*-nitrophenolate was monitored at 405 nm, using a 96-well microplate reader (SpectraMax ABS, USA). All the experiments were repeated three times in a triplicate manner.  $\text{KH}_2\text{PO}_4$  was used as the reference inhibitor of CIALP.

The Alkaline Phosphatase activities were calculated according to the following formula:

$$\text{Alkaline Phosphatase activity (\%)} = (\text{OD}_{\text{control}} - \text{OD}_{\text{sample}} \times 100) / \text{OD}_{\text{control}}$$

$$(\%) \text{ of Hemolysis} = \frac{\text{Absorbance of Sample} - \text{Absorbance of Negative Control}}{\text{Absorbance of Positive Control}} \times 100.$$

**Kinetic mechanism analysis.** Based on the  $\text{IC}_{50}$  results we select the most potent inhibitor (**Va**) for determine the mechanism of enzyme inhibition by following our reported method [33]. The inhibitor concentrations were used 0.00, 0.531 and 1.062  $\mu\text{M}$ . Substrate *p*-NPP concentrations were 10, 5, 2.5, 1.25, 0.625 and 0.3125 mM. Pre-incubation time and other conditions were same as described in alkaline phosphatase inhibition assay section. Maximal initial velocities were determined from initial linear portion of absorbances up to 10 minutes after addition of enzyme at per minute's interval. The inhibition type on the enzyme was assayed by Lineweaver-Burk plot of inverse of velocities ( $1/V$ ) versus inverse of substrate concentration  $1/[S]$   $\text{mM}^{-1}$ . The EI dissociation constant  $K_i$  was determined by secondary plot of  $1/V$  versus inhibitor concentration.

**Docking methodology.** The compounds were docked to the crystal structure of human placental alkaline phosphatase (PLAP) (PDB ID: 1ZED, resolution 1.57 Å), [18] which was obtained from the Protein Data Bank (PDB) [34, 35]. The Scigress Ultra version FJ 2.6 program [36] was used to prepare the crystal structure for docking, i.e., hydrogen atoms were added and crystallographic water molecules were removed. The Scigress software suite was also used to build the inhibitors and the MM2 [37] force field was used to optimise the structures. The centre of the binding pocket was defined as the nitrogen atom of the co-crystallized ligand 4-nitrophenyl hydrogen methylphosphonate with the coordinates ( $x = 33.351$ ,  $y = 12.865$ ,  $z = 12.025$ ) with 10 Å radius, which is in close proximity to the side chains of Arg166 and His432. Fifty docking runs were allowed for each ligand with default search efficiency (100%). The basic amino acids lysine and arginine were defined as protonated. Furthermore, aspartic and glutamic acids were assumed to be deprotonated. The GoldScore (GS), [23] ChemScore (CS), [38, 39], Chem Piecewise Linear Potential (ChemPLP) [40], and Astex Statistical

Where  $\text{OD}_{\text{control}}$  and  $\text{OD}_{\text{sample}}$  represents the optical densities in the absence and presence of sample, respectively.

**Hemolytic assay.** Bovine blood samples were taken for the formation of RBCs suspension following already reported method [31, 32]. Solution (10 mg/mL, 20  $\mu\text{L}$ ) of synthesized compound was incubated with 180  $\mu\text{L}$  of red blood cells suspension at room temperature. Triton 100-X and PBS was used as positive and negative control respectively. Percentage of hemolysis was calculated by following formula:

Potential (ASP) [41] scoring functions were implemented to validate the predicted binding modes and relative energies of the ligands using the GOLD v5.7.3 software suite. The QikProp 10.2 [42], software package was used to calculate the molecular descriptors of the compounds. The reliability of QikProp is established for the molecular descriptors [43].

## CONCLUSION

*N*-(Substituted-phenyl)-3-(4-phenyl-1-piperazinyl)propanamides (**Va-e**) were synthesized in good yields and their structures were corroborated by spectral (FT-IR,  $^1\text{H-NMR}$ ,  $^{13}\text{C-NMR}$ , HMBC) and CHN analysis data. All synthesized compounds possessed remarkable alkaline phosphate enzyme inhibition as it was depicted by their lower  $\text{IC}_{50}$  values relative to standard used. Moreover, all these molecules were attributed with low cytotoxicity and therefore, might serve as valuable therapeutic agents for alkaline phosphatase-associated disorders, particularly, bone diseases, diabetes, prostatic cancer and liver dysfunction.

## ACKNOWLEDGMENTS

We highly acknowledge the Higher Education Commission (HEC) of Pakistan for providing the financial support for spectroscopic facilities.

## COMPLIANCE WITH ETHICAL STANDARDS

This article does not contain any studies involving human participants performed by any of the authors and does not contain any studies involving animals performed by any of the author.

## Conflict of Interests

All authors declare that they have no conflict of interest.

## SUPPLEMENTARY INFORMATION

The online version contains supplementary material available at <https://doi.org/10.1134/S1068162021050186>.

## REFERENCES

- Kharb, R., Shaharyar, M., and Sharma, P.C., *Curr. Med. Chem.*, 2011, vol. 18, no. 21, pp. 3265–3297. <https://doi.org/10.2174/092986711796391615>
- Kerns, R.J., Rybak, M.J., Kaatz, G.W., Vaka, F., Cha, R., Grucz, R.G., and Diwadkar, V.U., *Bioorg. Med. Chem. Lett.*, 2003, vol. 13, pp. 2109–2112. [https://doi.org/10.1016/S0960-894X\(03\)00376-7](https://doi.org/10.1016/S0960-894X(03)00376-7)
- Kimura, M., Masuda, T., Yamada, K., Mitani, M., Kubota, N., Kawakatsu, N., Kishii, K., Inazu, M., Kiuchi, Y., Oguchi, K., and Namiki, T., *Bioorg. Med. Chem.*, 2003, vol. 11, pp. 3953–3963. [https://doi.org/10.1016/S0968-0896\(03\)00428-0](https://doi.org/10.1016/S0968-0896(03)00428-0)
- Kharb, R., Bansal, K., and Sharma, A.K., *Der Pharma Chemica.*, 2012, vol. 4, no. 6, pp. 2470–2488. <https://www.derpharmachemica.com/pharma-chemica/a-valuable-insight-into-recent-advances-on-anti-microbial-activity-of-piperazine-derivatives.pdf>
- Faist, J., Seebacher, W., Saf, R., Brun, R., Kaiser, M., and Weis, R., *Eur. J. Med. Chem.*, 2012, vol. 47, no. 1, pp. 510–519. <https://doi.org/10.1016/j.ejmech.2011.11.022>
- Dorsey, B.D., McDonough, C., McDaniel, S.L., Levin, R.B., Newton, C.L., Hoffman, J.M., Darke, P.L., Zugay-Murphy, J.A., Emini, E.A., Schleif, W.A., Olsen, D.B., Stahlhut, M.W., Rutkowski, C.A., Kuo, L.C., Lin, J.H., Chen, W., Michelson, S.R., Holloway, M.K., Huff, J.R., and Vacca, J.P., *J. Med. Chem.*, 2000, vol. 43, pp. 3386–3399. <https://doi.org/10.1021/jm9903848>
- Chandra, J.N.N.S., Sadashiva, C.T., Kavitha, C.V., and Rangappa, K.S., *Bioorg. Med. Chem.*, 2006, vol. 14, no. 19, pp. 6621–6627. <https://doi.org/10.1016/j.bmc.2006.05.064>
- Chaudhary, S., Verma, H.C., Gupta, M.K., Gupta, R.K., Kumar, A., and El-Shorbagi, A.N., *Asian J. Pharm. Clin. Res.*, 2019, vol. 12, pp. 310–315. <https://doi.org/10.22159/ajpcr.2019.v12i1.30094>
- Aziz-ur-Rehman, Ahtaz, N., Abbasi, M.A., Zahra, S.Z., Saleem, S., Manzoor, S., Iqbal, J., Virk, N.A., and Chohan, T.A., *Trop. J. Pharm. Res.*, 2018, vol. 17, no. 6, pp. 1145–1153. <https://doi.org/10.4314/tjpr.v17i6.22>
- Khalifa, M.M.A., Baset, M.A., and El-Eraky, W., *Med. Chem. Res.*, 2012, vol. 21, no. 12, pp. 4447–4454. <https://doi.org/10.1007/s00044-012-9983-3>
- Rapacz, A., Kaminski, K., Obniska, J., Koczurkiewicz, P., Pekala, E., and Filippek, B., *Naunyn-Schmiedeberg's Arch. Pharmacol.*, 2017, vol. 390, no. 6, pp. 567–579. <https://doi.org/10.1007/s00210-017-1358-3>
- Kusuma, B., and Gade, D., *Int. J. Pharm. Bio. Sci.*, 2018, vol. 8, no. 3, pp. 1154–1161. [https://www.ijpbs.com/ijpbsadmin/upload/ijpbs\\_5c2c74155dd3b.pdf](https://www.ijpbs.com/ijpbsadmin/upload/ijpbs_5c2c74155dd3b.pdf)
- McComb, R.B., Bowers, G.N., and Posen, S., *Alkaline phosphatase*, 1979, pp. 289–372. [https://link.springer.com/chapter/10.1007/978-1-4613-2970-1\\_7](https://link.springer.com/chapter/10.1007/978-1-4613-2970-1_7)
- Kim, E.E., and Wyckoff, H.W., *J. Mol. Biol.*, 1991, vol. 218, no. 2, pp. 449–464. [https://doi.org/10.1016/0022-2836\(91\)90724-k](https://doi.org/10.1016/0022-2836(91)90724-k)
- Stec, B., Holtz, K.M., and Kantrowitz, E.R., *J. Mol. Biol.*, 2000, vol. 299, no. 5, pp. 1303–1311. <https://doi.org/10.1006/jmbi.2000.3799>
- De-Backer, M.M.E., McSweeney, S., Lindley, P.F., and Hough, E., *Acta Crystallogr. Sect. D: Biol. Crystallogr.*, 2004, vol. 60, no. 9, pp. 1555–1561. <https://doi.org/10.1107/S0907444904015628>
- Le-Du, M.H., Stigbrand, T., Taussig, M.J., Menez, A., and Stura, E.A., *J. Biol. Chem.*, 2001, vol. 276, no. 12, pp. 9158–9165. <https://doi.org/10.1074/jbc.m009250200>
- Llinas, P., Stura, E.A., Menez, A., Kiss, Z., Stigbrand, T., Millaan, J.L., and Le-Du, M.H., *J. Mol. Biol.*, 2005, vol. 350, no. 3, pp. 441–451. <https://doi.org/10.1016/j.jmb.2005.04.068>
- Kang, E.B., Choi, C.A., Mazrad, Z.A.I., Kim, S.H., In, I., and Park, S.Y., *Anal. Chem.*, 2017, vol. 89, no. 24, pp. 13508–13517. <https://doi.org/10.1021/acs.analchem.7b03853>
- Li, S.J., Li, C.Y., Li, Y.F., Fei, J., Wu, P., Yang, B., Ou-Yang, J., and Nie, S.X., *Anal. Chem.*, 2017, vol. 89, no. 12, pp. 6854–6860. <https://doi.org/10.1021/acs.analchem.7b01351>
- Tang, Z., Zhang, H., Ma, C., Gu, P., Zhang, G., Wu, K., Chen, M., and Wang, K., *Microchim. Acta.*, 2018, vol. 185, p. 109. <https://link.springer.com/article/10.1007/s00604-017-2628-y>
- Zhao, J.H., Wang, S., Lu, S., Bao, X., Sun, J., and Yang, X., *Anal. Chem.*, 2018, vol. 90, no. 12, pp. 7754–7760. <https://doi.org/10.1021/acs.analchem.8b01845>
- Jones, G., Willet, P., Glen, R.C., Leach, A.R., and Taylor, R., *J. Mol. Biol.*, 1997, vol. 267, pp. 727–748. <https://doi.org/10.1006/jmbi.1996.0897>
- Miliutina, M., Ejaz, S.A., Khan, S.U., Iaroshenko, V.O., Villinger, A., Iqbal, J., and Langer, P., *Eur. J. Med. Chem.*, 2017, vol. 126, pp. 408–420. <https://doi.org/10.1016/j.ejmech.2016.11.036>
- Al-Rashida, M., Ejaz, S.A., Ali, S., Shaikat, A., Hamayoun, M., Ahmed, M., and Iqbal, J., *Bioorg. Med. Chem.*, 2015, vol. 23, no. 10, pp. 2435–2444. <https://doi.org/10.1016/j.bmc.2015.03.054>
- Borosky, G.L., and Lin, S., *J. Chem. Inf. Mod.*, 2011, vol. 51, no. 10, pp. 2538–2548. <https://doi.org/10.1021/ci200228s>
- Zhu, F., Logan, G., and Reynisson, J., *Mol. Inf.*, 2012, vol. 31, pp. 847–855. <https://doi.org/10.1002/minf.201200103>
- Hussain, G., Abbasi, M.A., Aziz-ur-Rehman, Siddiqui, S.Z., Ahmad, I., Malik, R., Shahid, M., Mush-taq, Z., and Shah, S.A.A., *Trop. J. Pharm. Res.*, 2018, vol. 17, no. 7, pp. 1397–1406. <https://doi.org/10.4314/tjpr.v17i7.25>
- Iqbal, Z., Ashraf, Z., Hassan, M., Abbas, Q., and Ja-been, E., *Bioorg. Chem.*, 2019, vol. 90, pp. 103–108. <https://doi.org/10.1016/j.bioorg.2019.103108>
- Ur-Rehman, S., Saeed, A., Saddique, G., Channar, P.A., Larik, F.A., Abbas, Q., Hassan, M., Raza, H., Fattah, T.A., and Seo, S.Y., *Bioorg. Med. Chem.*, 2018, vol. 26,

- pp. 3707–3715.  
<https://doi.org/10.1016/j.bmc.2018.06.002>
31. Shahid, M., Bukhari, S.A., Gul, Y., Munir, H., Anjum, F., Zuber, M., Jamil, T., and Zia, K.M., *Int. J. Bio. Macro.*, 2013, vol. 62, pp. 172–179.  
<https://doi.org/10.1016/j.ijbiomac.2013.08.018>
  32. Yang, C.R. Zhang, Y., Jacob, M.R., Khan, S.I., Yhang, Y.J., and Li, X.C., *Chemotherapy.*, 2006, vol. 50, pp. 1710–1714.  
<https://dx.doi.org/10.1128%2FAAC.50.5.1710-1714.2006>
  33. Abbasi, M.A., Nazir, M., Aziz-ur-Rehman, A., Siddiqui, S.Z., Hassan, M., Raza, H., Shah, S.A., Shahid, M., and Seo, S.Y., *Arch. Pharm.*, 2019, vol. 352, p. 1800278.  
<https://doi.org/10.1002/ardp.201800278>
  34. Berman, H.M., Westbrook, J., Feng, Z., Gilliland, G., Bhat, T.N., Weissig, H., Shindyalov, I.N., and Bourne, P.E., *Nucleic Acids Res.*, 2000, vol. 28, pp. 235–242.  
<https://doi.org/10.1093/nar/28.1.235>
  35. Berman, H., Henrick, K., and Nakamura, H., *Nat. Struct. Biol.*, 2003, vol. 10, pp. 980.  
<https://doi.org/10.1038/nsb1203-980>
  36. Scigress *Scigress: Version FJ 2.6 (EU 3.1.7)*, Fijitsu Limited: 2008–2016.
  37. Allinger, N.L., *J. Am. Chem. Soc.*, 1977, vol. 99, pp. 8127–8134.  
<https://doi.org/10.1021/ja00467a001>
  38. Eldridge, M.D., Murray, C., Auton, T.R., Paolini, G.V., and Mee, R.P., *J. Comp. Aid. Mol. Design*, 1997, vol. 11, pp. 425–445.  
<https://doi.org/10.1023/a:1007996124545>
  39. Verdonk, M.L., Cole, J.C., Hartshorn, M.J., Murray, C.W., and Taylor, R.D., *Proteins*, 2003, vol. 52, no. 4, pp. 609–623.  
<https://doi.org/10.1002/prot.10465>
  40. Korb, O., Stutzle, T., and Exner, T.E., *J. Chem. Inf. Model.*, 2009, vol. 49, no. 1, pp. 84–96.  
<https://doi.org/10.1021/ci800298z>
  41. Mooij, W.T.M., and Verdonk, M.L., *Proteins*, 2005, vol. 61, no. 2, pp. 272–287.  
<https://doi.org/10.1002/prot.20588>
  42. QikProp, Schrodinger, LLC, New York, NY, 2017.
  43. Ioakimidis, L., Thoukydidis, L., Naeem, S., Mirza, A., and Reynisson, J., *QSAR Comb. Sci.*, 2008, vol. 27, pp. 445–456.  
<https://doi.org/10.1002/qsar.200730051>